JCTC Journal of Chemical Theory and Computation

Article

pubs.acs.org/JCTC

Density-Difference-Driven Optimized Embedding Potential Method To Study the Spectroscopy of Br_2 in Water Clusters

Octavio Roncero,*[,†] Alfredo Aguado,[‡] Fidel A. Batista-Romero,[¶] Margarita I. Bernal-Uruchurtu,[¶] and Ramón Hernández-Lamoneda[¶]

[†]Instituto de Física Fundamental (IFF-CSIC), C.S.I.C., Serrano 123, 28006 Madrid, Madrid, Spain

[‡]Departamento de Química Física Aplicada (UAM), Unidad Asociada a IFF-CSIC, Facultad de Ciencias Módulo 14, Universidad Autónoma de Madrid, 28049 Madrid, Madrid, Spain

[¶]Centro de Investigaciones Químicas, Universidad Autónoma del Estado de Morelos, Cuernavaca, Morelos, México 62209

ABSTRACT: A variant of the density difference driven optimized embedding potential (DDD-OEP) method, proposed by Roncero et al. (*J. Chem. Phys.* **2009**, *131*, 234110), has been applied to the calculation of excited states of Br_2 within small water clusters. It is found that the strong interaction of Br_2 with the lone electronic pair of the water molecules makes necessary to optimize specific embedding potentials for ground and excited electronic states, separately and using the corresponding densities. Diagnosis and convergence studies are presented with the aim of providing methods to be applied for the study of chromophores in solution. Also, some preliminary results obtained for the study of electronic states of Br_2 in clathrate cages are presented.

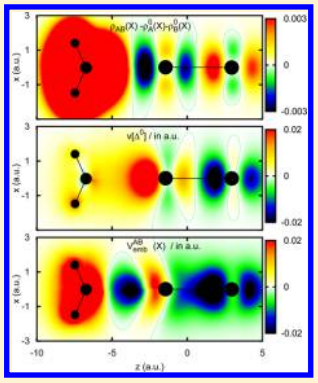

1. INTRODUCTION

The spectroscopic behavior of halogens has intrigued scientists for more than a century. These diatomic molecules have a rich valence electronic spectra in the visible region that is quite sensitive to the environment. In recent years the electronic spectra of Br_2 has received some attention due to the interesting differences found on it in different aqueous environments.

The motivation of this work stems from the electronic spectra of Br_2 in clathrate cages which have been studied experimentally by Janda, Apkarian, and co-workers.[1−3] The $Br_2(X \rightarrow B,C)$ excitation spectrum in gas phase consists of two broad bands which overlap, showing a maxima and a shoulder at ≈21000 and 24000 cm^{-1}, respectively, which approximately correspond to the vertical excitation from the equilibrium configuration of $Br_2(X)$ toward the B and C states above their dissociation asymptote.[4]

The amount these bands are shifted in clathrate hydrates seems to be strongly dependent on the type of cage where the dihalogen is trapped.[3] Usually these shifts are of the order of 100−1000 cm^{-1}. Gas hydrate crystals are formed by combinations of cages of different sizes, and the X-ray diffraction experiments[5−7] on chlorine and bromine hydrates are not simple to interpret. As a first step to test the present methodology, we shall start studying the $Br_2-(H_2O)_n$ clusters (with n = 1 and 5) as benchmark systems where methods designed for large systems can be applied and compared with highly accurate *ab initio* methods.[3]

The calculation of excited electronic states on large systems is nowadays a theoretical challenge. One possible alternative is the use of a time-dependent density functional theory (TD-DFT) based on the Runge and Gross theorem.[8] Numerous examples on the application of TD-DFT to study the electronic spectroscopy of large systems are now available.[9] These methods, however, are subject to the common problems of DFT, such as self-interaction and are usually not accurate to reproduce electronic excited states with spectroscopic accuracy.

The study of electronic spectroscopy of nonperiodic large systems, as biomolecules, have increasingly been studied partitioning the (unaffordable) whole system into two or more parts, the chromophore, A, and the environment, B. The coupling between the two subsystems can be treated in many different ways, from entirely quantum schemes, to diverse combinations of molecular dynamics and quantum approaches.[10−12] A popular method of this kind consists of using ab initio quantum chemistry methods for studying the A subsystem, embedded in the classical force-field of the environment, the so-called QM/MM methods.[13,14] In these models polarizable and not polarizable force fields are used to describe the mutual polarization of the A (QM) and B (MM) regions, in which the classical surroundings are described by static electric multipoles and induced dipoles.[15] However, these multiscale models are often not accurate enough, and more complex partition models have to be developed in order to

Received: December 17, 2014
Published: February 6, 2015

DOI: 10.1021/ct501140p
J. Chem. Theory Comput. 2015, 11, 1155−1164

account for the mutual active/environment interaction beyond pure electrostatic forces.[16]

A further improvement is achieved by obtaining the "embedding" potentials using DFT techniques to describe the interaction of a subsystem and its environment.[17−19] A very successful method is the so-called frozen density embedding (FDE) approach of Wesolowski and Warshel.[19] In this density-functional embedding theory, the density of the whole system and that of the "active" cluster A are first obtained from DFT calculations, and the embedding potential is derived from them iteratively, by minimizing the interaction energy between the two subsystems described by approximate kinetic and exchange functionals. In this approach the environment was kept frozen, giving rise to the name of the method, but little after a refinement was introduced allowing its optimization.[20] This method has been applied to many large systems using DFT-in-DFT techniques and different approaches for the environment.[16,19,21−23] In addition, an intensive work has been devoted to improve this method for treating electronic correlation using multideterminantal wave functions[24] and analyzing the effect of different functionals used for the kinetic energy term.[25−29] In this formalism the excited electronic states can be described using the corresponding time-dependent embedding potential theory.[30−33]

Carter and co-workers[34−37] proposed to extend this formalism to perform *ab initio* wave function based calculations on the A subsystem, by using the embedding potential obtained with the FDE approach.[19] This is done by adding the monoelectronic embedding potential to the Fock operator leading to a modified Hartree−Fock (MHF) equation. Using this MHF operator it is therefore possible to use any conventional *ab initio* method, including electron correlation effects, giving rise to the so-called WFT-in-DFT methods.[38−41] This procedure allows the calculation of accurate excited electronic states and has been widely used.[16,42]

The approximate character of the kinetic energy functional is a subject of continuous research on the FDE approach and is one of the weaknesses of these methods.[26,28,34−36] To avoid the use of kinetic energy functional, the optimized embedding potential (OEP) methods have been proposed,[43] in which the embedding potential is obtained by an inversion procedure minimizing the density difference $\rho_A^{ref}-\rho_A$, where ρ_A^{ref} is a reference density for subsystem A in the whole system and ρ_A is obtained from the MHF equation for the A subsystem with the optimized embedding potential. Different optimization procedures have been proposed, iteratively using the Zhao-Morrison-Parr self-repulsion potential[43] as previously proposed to obtain exact DFT functionals,[44] combining the King-Handy expression for the exact kinetic potential[45] or using a direct method[29] previously proposed by Wu and Yang.[46] This method is closely related to those used in DFT to "invert" the exchange correlation potential from the "exact" electronic density method.[44,47−54] To avoid the optimization procedure, Manby et al. have proposed recently to use a projection technique enforcing Pauli exclusion to get the embedding potential.[55]

In the above-mentioned OEP method one problem is the determination of the ρ_A^{ref} reference density, usually done with projection techniques. In ref 43, ρ_A^{ref} was obtained using the Mulliken method and therefore was not v-representable. To overcome this problem, Roncero et al. proposed a OEP method in which the total density is partitioned by minimizing $\rho-\rho_A-\rho_B$, where ρ_A and ρ_B are densities obtained from MHF equations modified by embedding potentials, one for each subsystem, which were iteratively obtained[56] using the density difference as a driving force. This density difference driven optimized embedding potential (DDD-OEP) method guarantees the v-representability of the densities for the two subsystems.

Later, it was demonstrated that if the embedding potential exists, it should be unique for all subsystems.[57] This is connected to a similar conclusion arising the partition density functional theory (PDFT)[58−60] arising from a common minimization of the reference energy. This uniqueness issue is a fundamental one in the development of methods to obtain embedding potentials. Here, however, we follow a heuristic procedure based on this statement.

In this work we shall used the DDD-OEP method of ref 56, slightly modified to consider a common embedding potential contribution for A and B, plus an extra perturbative polarization term independent for A and B. This method is described in section II, and it is applied to the study of the electronic spectra of Br_2 in several $(H_2O)_n$ clusters (n = 1 and 5), used as a benchmark to check the accuracy of the method. This study will focus on the need of using several state-dependent embedding potentials to accurately describe the vertical excitation toward excited electronic states as recently proposed by Daday et al.,[42] described in section III. A diagnosis will be made on whether or not it is necessary to use one or several state-dependent embedding potentials. Section IV will be devoted to extract some conclusions, showing some preliminary results obtained for Br_2 inside a clathrate formed by 24 water molecules.

2. DENSITY-DIFFERENCE-DRIVEN OPTIMIZED EMBEDDING POTENTIAL (DDD-OEP) METHOD

Let us consider that the density ρ of the total AB system is known. In general, for large systems it will be obtained by a monodeterminantal DFT method or similar, but there is not any formal restriction to use any desired method. The aim of the OEP methods is to partition this density as

$$\rho = \rho_A + \rho_B \tag{1}$$

such that ρ_A and ρ_B are v-representable. This is warranted by obtaining them from MHF equations of the type

$$[\hat{\mathcal{F}}_C + \hat{\mathcal{V}}_C]\phi_{C,l} = \epsilon_{C,l}\phi_{C,l} \tag{2}$$

where $C = A$ or B denotes the subsystem, and l is a quantum number specifying the molecular orbital $\phi_{C,l}$ of C subsystem with energy $\epsilon_{C,l}$. $\hat{\mathcal{F}}_C$ and $\mathcal{V}_C$ are the Fock operator and the embedding potential for subsystem C, respectively.

Following ref 57, the embedding potential should be unique, *i.e.*, $\mathcal{V}_A = \mathcal{V}_B$. In this work we shall consider a slight correction to this restriction, by setting two contributions

$$\mathcal{V}_C = \mathcal{V} + \mathcal{P}_C \tag{3}$$

where $\mathcal{V}$ is a common dividing contribution which is the main component of the whole embedding potential. $\mathcal{P}_C$ is an extra polarization term which is added to each subsystem C to improve the accuracy of eq 1 by reasons which will be clarified below. This $\mathcal{P}_C$ is added as second-order corrections to the final embedding potential once the best $\mathcal{V}$ is obtained and do not modify it qualitatively, and in some OEP methods or similar it is neglected.[57−60]

DOI: 10.1021/ct501140p
J. Chem. Theory Comput. 2015, 11, 1155−1164

$\mathcal{V}$ can be obtained by applying a direct inversion method.[29,45,57] Here we shall use a variant of the iterative procedure developed previously,[43,56] as

$$\mathcal{V}_C^{k+1} = \mathcal{V}_C^k + \lambda v^k[\Delta^k] \tag{4}$$

where λ is a parameter which minimizes δ^k at each iteration k. This δ^k is a measure of the density difference defined as

$$\delta^k = \int d\mathbf{r}(\Delta^k)^2 = \mathrm{Tr}[\mathbf{S}\Delta^k\mathbf{S}\Delta^k] \tag{5}$$

where $\mathbf{S}$ is the overlap matrix and

$$\Delta^k = \rho - (\rho_A^k + \rho_B^k) \tag{6}$$

is the density difference at iteration k, where ρ_A^k and ρ_B^k are densities obtained from the resolution of the MHF equation, eq 2, where $\hat{\mathcal{V}}_C$ is substituted by its value at iteration k, denoted $\mathcal{V}_C^k$.

In the first iteration $\mathcal{V}_C^k = 0$ and $\rho_C{}^0$ are the densities of the isolated A and B subsystems. As an example, the density difference Δ^0 obtained for the $H_2O{-}Br_2(X)$ complex is shown in the top panel of Figure 1. It presents positive and negative

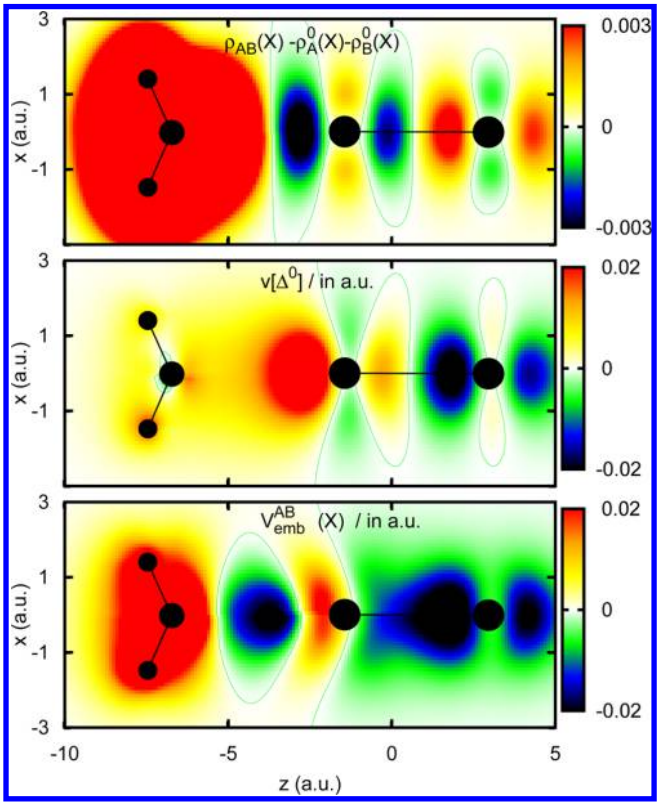

Figure 1. Density difference for $k = 0$ (top panel), self-repulsion potential v_{rep}^k, eq 8 (middle panel), and embedding potential $\mathcal{V}^{k=150}$ obtained for the $H_2O{-}Br_2$ complex at a distance $R = 4$ Å, with the two Br atoms and O along the z-axis, as indicated in the figure, while the two H atoms are out of the x-z plane in a nonsymmetric configuration.

values. Positive values are associated with regions where $\rho > \rho_A^k + \rho_B^k$, and the embedding potential should therefore be negative to "attract" electronic density to fill this density deficit. On the contrary at the negative regions, $\rho < \rho_A^k + \rho_B^k$, and some density has to be removed in those regions, which is achieved by making the embedding potential repulsive. It can therefore be said that the density difference Δ^k can be used as a driving force to design the embedding potential or, equivalently, that the embedding potential is a functional of the density difference, as indicated in eq 4.

In the ZMP procedure[44] and in the OEP method,[43] the self-repulsion potential, $v^k[\Delta_C^k]$, appearing in eq 4 was defined as

$$v^k[\Delta^k] = -\int d\mathbf{r}\,\frac{\Delta^k}{\mathbf{r} - \mathbf{r}'} \tag{7}$$

Such potential corresponds to the electric field arising from the density difference Δ^k and introduces a driving force to make $\rho_A^k + \rho_B^k$ coincide with the reference density ρ. However, in ref 56 it was found that it is more efficient to substitute the Coulomb self-repulsion potential, eq 7, by the exchange self-repulsion potential defined in the atomic basis set representation as a matrix whose elements are given by

$$v_{i,j}^k[\Delta^k] = \frac{1}{2}\sum_{m,l}\Delta_{m,l}^k(imlj) \tag{8}$$

where $\Delta_{i,j}^k$ are the matrix elements of Δ^k, and $(imlj)$ denotes the bielectronic matrix elements among the atomic basis functions. This self-repulsion term is shown in the middle panel of Figure 1 for the initial iteration, $k = 0$, and it shows an oscillatory behavior similar to the density difference Δ^0, but with the opposite sign. This is the expected behavior of the functional required to represent the embedding potential. The ability of the self-repulsion potential to drive the sum $\rho_A^k + \rho_B^k$ is demonstrated by the fact that the final embedding potential obtained, in the bottom panel of Figure 1, is very close to $v_{rep}^{k=0}$, in the middle panel.

The procedure followed in this work to construct the total embedding potential $\mathcal{V}_A$ and $\mathcal{V}_B$ consists of two sequential iterative procedures, one to obtain the common dividing potential $\mathcal{V}$, and the second to calculate the polarization contributions $\mathcal{P}_A$ and $\mathcal{P}_B$, which is only done if the $\delta^k > \epsilon$ in the final step of the first iterative procedure.

To summarize, the first iterative procedure consists of the following steps:

1. ρ_A^k and ρ_B^k are obtained, by any method consistent with the method used to get the total ρ, HF, DFT, or any other like MC-SCF used here to calculate the triplet states described below.

2. The density difference, Δ^k, is evaluated and with it the exchange self-repulsion potential, v^k, using eq 8. These quantities are calculated in the present implementation in the MOLPRO package using the MATROP utilities.

3. The MHF equation is solved for subsystem A and B, for several values of λ. A minimization of δ^k is done as a function of the λ parameter using the SIMPLEX code implemented in MOLPRO. Once this value is found, λ_{min}, it is used to construct the embedding potential $\mathcal{V}^{k+1}$ following eq 4.

4. If $\delta^k < \delta^{k-1}$ and $\delta^k > \epsilon$ ($\epsilon = 10^{-5}$ in the present case) the process goes back to step 1. Otherwise this first iterative procedure is stopped. A maximum number of iterations ($k_{max} = 150$ in this case) is imposed, to avoid an unnecessarily high number of iterations, as usually done in any self-consistent procedure. Morever, if in a given loop $\delta^k > \delta^{k-1}$ and no improvement is found, the optimization procedure is also stopped. Sometimes, specially for short distances, the density difference δ^k cannot be reduced to a desired value simply because the densities are not separable. This is for example the case for $R = 3.4$ in Figure 2. However, the procedure may

DOI: 10.1021/ct501140p
J. Chem. Theory Comput. 2015, 11, 1155−1164

reduce the density difference in several order of magnitudes, from approximately $\delta^{k=0} = 1$ to $\delta^{k=300} < 0.005$ in the case mentioned.

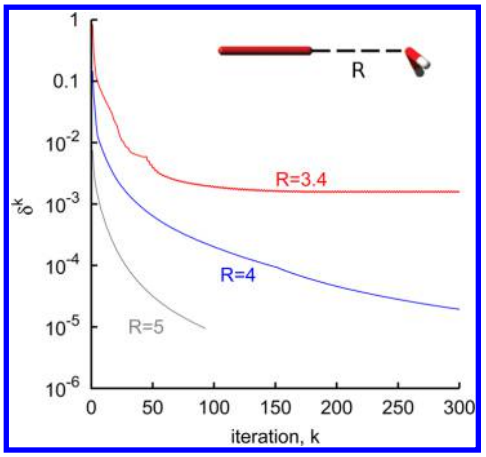

Figure 2. δ^k as a function of the iteration k obtained for $H_2O{-}Br_2(X)$ complex for three distances R (in Å) as indicated in the inset. For R = 5, the optimization is completed with only the first iterative procedure and $\mathcal{V}_A = \mathcal{V}_B$. For R = 3.4 Å, in the repulsive part of the potential, the first iterative procedure ends at k = 4, and it is continued with the second iterative procedure as explained in the text.

A typical example of the convergence is shown in Figure 2 for the $H_2O{-}Br_2(X)$ complex at several distances between the two monomers and the geometry indicated in the inset (hereafter denoted by geometry 1a). For long distance R = 5 Å, δ^k decreases monotonically getting a fast convergence, in which the density difference is reduced by more than 3 orders of magnitude. For short distances, R = 3.4 Å, this first iteration reaches a plateau at k = 44 from which the δ^k cannot be further reduced following this method.

Under these circumstances it is convenient to relax the uniqueness of the embedding potential and consider the polarization contributions, $\mathcal{P}_A$ and $\mathcal{P}_B$, arising from the mutual interaction between them. Since the density difference has been reduced by more than 2 orders of magnitude in the worst case, these new corrections are considerably smaller and can be considered as small perturbative corrections added to reduce even more the density difference or more specifically δ^k.

In the second iterative process, we follow the procedure outlined in ref 56 starting from the last $\mathcal{V}^{k_{max}}$ and $\rho_B^{k_{max}}$ obtained in the first iterative procedure and consisting of the following steps:

1. The new Δ^{k+1} is evaluated and from it the self-repulsion potential, v^{k+1}, using eq 8.
2. The MHF equation is solved for subsystem A only, minimizing δ^{k+1} as described above, finding λ_{min}^A, to build the embedding potential $\mathcal{V}_A^{k+1} = \mathcal{V}^{k_{max}} + \lambda_{min}^A v^{k+1}$, and the MHF eq 2 is solved for A, determining ρ_A^{k+1}.
3. A new density difference is set, Δ^{k+2}, and with it a new exchange self-repulsion potential, $v_{i,j}^{k+2}$, is obtained.
4. The MHF equation is solved for subsystem B, minimizing δ^{k+2} as described above for A subsystem, and constructing $\mathcal{V}_B^{k+2}$.
5. If the $\delta^{k+2} < \epsilon$ or $\delta^{k+2} > \delta^k$ the procedure is stopped. Otherwise, another loop is started from point 2.

Adding this second iterative refinement, it is possible to decrease even more δ^k, as shown for R = 3.4 Å in Figure 2.

With the $\mathcal{V}_A = \mathcal{V}_A^{k'_{max}}$ potential thus determined, the resolution of the MHF equation is performed to obtain the molecular orbitals, the density ρ_A, and the Hartree−Fock energy $E_{A,HF}$. The orbitals $\phi_{A,l}^k$ are then used in a multireference configuration interaction (MRCI) calculation to obtain more accurate electronic energies $E_{A,CI}^i$, where i denotes the electronic excitation, i = 0 being the ground electronic state eigenvalue.

The correlation (i = 0) or excitation (i > 0) energies are determined as $E_{cor}^i = E_{A,CI}^i - E_{A,HF}$. The energy of the i electronic state of the total system AB is given by

$$E^i = E_{tot} + E_{cor}^i = E_{tot} + E_{A,CI}^i - E_{A,HF} \quad (9)$$

where E_{tot} is the energy obtained for the whole system AB. To avoid double-counting the correlation energy it is convenient to evaluate the HF energy associated with the density ρ, used as reference obtained for the total system AB, and replace E_{tot} by $E_{tot,HF}$.

3. STATE-SPECIFIC EMBEDDING POTENTIALS FOR $(H_2O)_N{-}Br_2$ COMPLEXES

3.1. Numerical Details. The calculations have been performed using the MOLPRO package.[61] Augmented correlation-consistent polarized (aVTZ) basis sets of Dunning[62] were used for O and H atoms. For Br atoms, the relativistic effective core potential (RECP) of the Stuttgart group[63] was used. The aVTZ basis is used for the valence electrons and is extended with a set of g functions, giving a final basis of 4s4p3d2f1g, used previously to describe the excited states of $Ne{-}Br_2$ complexes and the nonadiabatic couplings.[64]

Internally contracted multireference configuration interaction (MRCI) calculation were performed for $(H_2O)_n{-}Br_2(X,B,C)$ (n = 1 and 5) on the whole systems for different distances between $(H_2O)_n$ and Br_2, to use as benchmark to compare with. These calculations on the whole system are represented in the figures discussed below by solid circles. In contrast, the calculations performed on the Br_2 subsystem but using an embedding potential to describe the water molecules will be represented by open circles.

Some equilibrium geometries of the most stable isomers of $(H_2O)_n{-}Br_2(X)$ complexes reported in ref 3 were used, and then the distance between the $(H_2O)_n$ and $Br_2(X)$ was varied to analyze in detail the interaction potential, keeping all the other geometrical parameters fixed. For $H_2O{-}Br_2(X)$ the 1a and 1b conformers were chosen. Isomer 1a corresponds to the halogen bonded complex, in which O−Br−Br bonds lie along the z axis as indicated in Figure 2. The 1b isomer is a weaker complex and corresponds to a hydrogen-halogen stabilized structure, in which Br_2 approaches one H atom of the water molecule, as indicated in Figure 1 of ref 3. For the $(H_2O)_5{-}Br_2(X)$ the most stable 5a geometry was chosen, which presents two kind of bonds between Br_2 and two different water molecules, an O−Br halogen-bond and a H−Br hydrogen-halogen interaction (see Figure 5 of ref 3).

Two sets of calculations were done in each case, using two embedding potentials: $\mathcal{V}_A(X)$ obtained using the reference density of the whole system of the X state, $\rho(X)$, correlating to $Br_2(X^1\Sigma_g^+)$. The second one, $\mathcal{V}_A(B)$ is obtained using the density of the B state, $\rho(B)$, correlating to the $Br_2(B^3\Pi_{0u}^+)$. $\rho(X)$ was calculated using a HF method, while $\rho(B)$ was calculated

DOI: 10.1021/ct501140p
J. Chem. Theory Comput. 2015, 11, 1155−1164

using the Multi-Configuration Self-Consistent-Field (MC-SCF) method. For the A = Br_2 subsystem, HF calculations are performed for singlets and MC-SCF for triplets. For B = $(H_2O)_n$ all calculations were performed at the HF level and only for the ground singlet state.

The density difference is usually reduced more easily starting from a pure Hartree−Fock density. When using a method including electronic correlation the density becomes less easily factorized as a pure sum of densities. However, since the density is more accurate it is expected that this correlated density serves better as a reference density. Thus, even when the δ^k does not get as close to zero as in the pure Hartree−Fock case, we do think it improves the description of the environment. Some more work on this topic should be addressed in the future

3.2. H_2O−Br_2 Examples. The interaction energies obtained for the 1a isomer of the H_2O−Br_2 complex calculated for the whole system (solid circles) and two different embedding potentials (open circles), $\mathcal{V}_A(X)$ and $\mathcal{V}_A(B)$, are shown in Figure 3. In the lower panel are presented the ground state

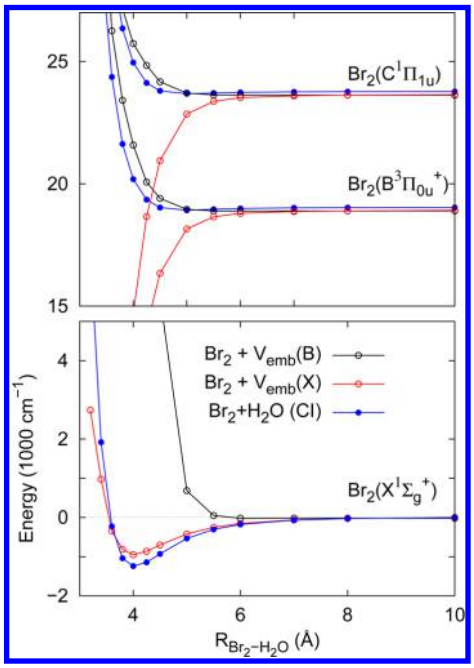

Figure 3. Energies calculated for the 1a isomer of H_2O−Br_2 as a function of the distance R (in Å) for the whole system, with solid circles, and for only Br_2 using the embedding potentials $\mathcal{V}_A(X)$ and $\mathcal{V}_A(B)$, obtained from $\rho(X)$ and $\rho(B)$, respectively. In the lower panel the results obtained for the ground singlet, X, are shown, and in the top panel the results obtained for the B and C state, as indicated in the figures.

potentials correlating to $Br_2(X^1\Sigma^+)$ and corresponding to a $\sigma_g^2\sigma_u^2\sigma_g^2\pi_u^4\pi_g^4$ configuration (see Figure 4). In the bottom of Figure 3 the results obtained with $\mathcal{V}_A(X)$ for the ground electronic state are presented, showing a good agreement with those coming from the whole system calculation. On the contrary, those obtained using $\mathcal{V}_A(B)$ fail to reproduce the attractive well and become quite repulsive at ≈5.5 Å.

An opposite behavior is observed for the two excited states, $B^3\Pi_{0u}$ and $C\ ^1\Pi_{1u}$. These two electronic states correspond to an electronic configuration in which one electron is promoted from the HOMO π_g orbital to the LUMO σ_u. In this case, the

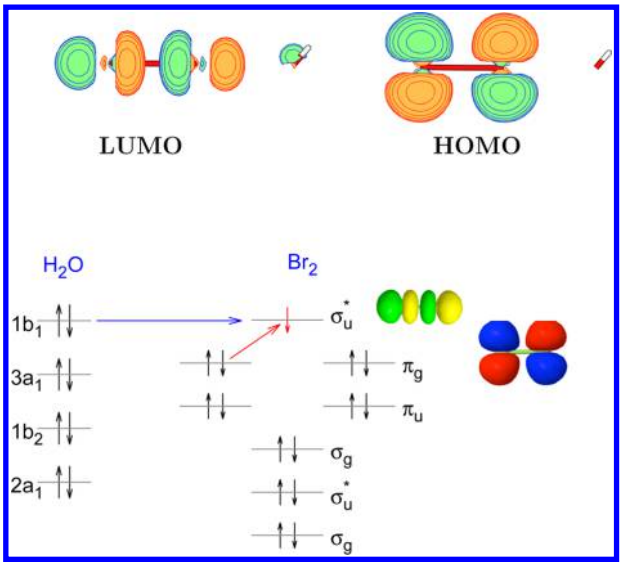

Figure 4. HOMO and LUMO orbitals involved in the ground and first excited states of the H_2O−Br_2(X,B,C) states.

results coming from $\mathcal{V}_A(B)$ are satisfactory, while those obtained with $\mathcal{V}_A(X)$ overestimate the binding energy becoming far too attractive. This is a clear indication that for this system, state-specific embedding potentials are needed to study the electronic excitation as recently used by Dadayet al.[42]

These results indicate that the electronic excitation not only is localized in Br_2 but also affects water molecule orbitals, specifically, the lone pair orbital on the oxygen atom. The force binding these two molecules, the halogen bond, is comparable in strength to a hydrogen bond and is a donor−acceptor interaction in which the dihalogen LUMO σ_u orbital accepts electronic density from the water molecule[65] and more specifically for water-bromine complexes[3](see Figure 4). In the H_2O−Br_2 complex the LUMO σ_u orbital is partially occupied by the lone pair of oxygen. Thus, when the system is excited by transferring one electron from the π_u HOMO orbital of Br_2 to the σ_u LUMO orbital, there is a significant change in the excitation energy because the LUMO orbital has already a fractional occupation.

It should be kept in mind that in the Br_2+$\mathcal{V}_A$ calculations, the electrons and charges of all water atoms are absent (in particular the lone pair of oxygen), but the atomic orbitals are included. $\mathcal{V}_A(X)$ presents an attractive region between Br_2 and O (see lower panel of Figure 1) leading the LUMO orbital of the Br_2+$\mathcal{V}_A(X)$ to be attracted to this region giving rise to excited electronic states with lower energies, as shown in the top panel of Figure 3. The difference between the two embedding potentials can be illustrated by the density differences Δ^0 obtained for the X and B electronic states, in Figure 5. The initial density difference obtained for the two cases is quite different, explaining the need of two different state-specific embedding potentials.

The 1b isomer of Br_2−H_2O complex characterized in ref 3 presents a shallower potential well than the 1a isomer in the ground electronic state. MRCI calculation of the 1b isomer of Br_2−H_2O yields ≈400 cm^{-1}, while that of the 1a isomer yields ≈1200 cm^{-1} for the respective well depths. In both cases it was found an important contribution of the dispersion forces,[3] being a third of the binding energy in the 1b case. This energy contribution needs to consider dynamical correlation to be

DOI: 10.1021/ct501140p
J. Chem. Theory Comput. 2015, 11, 1155−1164

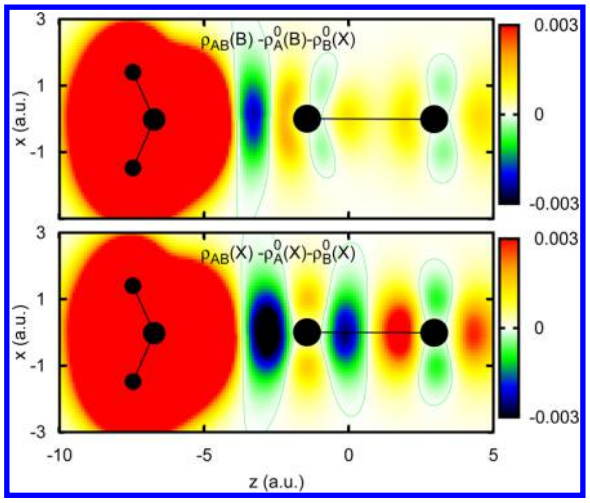

Figure 5. Density difference Δ^0 obtained for the 1a isomer of the H_2O-Br_2 complex at the minimum of the well for the X (bottom panel) and B (top panel) electronic states.

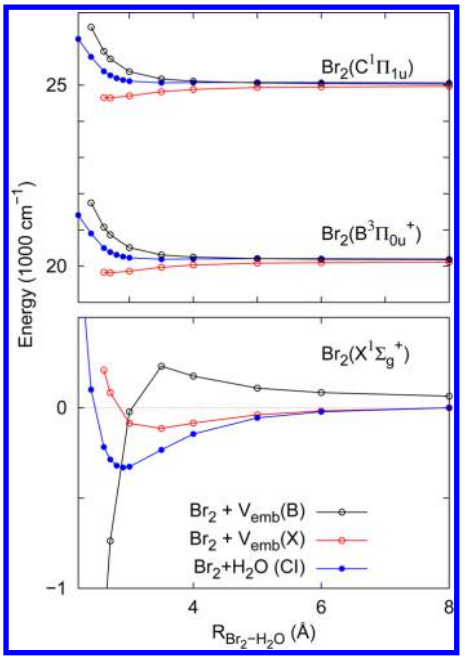

Figure 6. Energies calculated for the 1b isomer of H_2O-Br_2 as a function of the distance R (in Å) for the whole system, with solid circles, and for only Br_2 using the embedding potentials $\mathcal{V}_A(X)$ and $\mathcal{V}_A(B)$, obtained from $\rho(X)$ and $\rho(B)$, respectively. In the lower panel the results obtained for the ground singlet, X, are shown, and in the top panel the results obtained for the B and C state, as indicated in the figures.

accounted for, considering the simultaneous excitation of electrons in A = Br_2 and B = H_2O subsystems. For this reason, the calculation of the A subsystem with only the electrons of the Br_2 subsystem cannot describe this interaction. To improve the description of the complex well depth, the E_{tot} contribution in eq 9 should be considered. This energy contribution corresponds to that associated with the whole AB density ρ_{AB}. In the present case we are using either HF or MC calculations which do not describe correctly the dispersion contributions since they do not treat adequately the electronic dynamical correlation. To improve it, a MRCI or CCSD calculation should be done, which is impractical in large systems. An alternative is to use DFT functionals specially designed to describe van der Waals interactions.[66] Here we focus our attention on the electronic excitation energy and leave this problem for future analysis. It should be noticed, however, that in previous application of this embedding method it was possible to describe very weak van der Waals interaction between a H_2 molecule and a H_{10} chain. This was possible by considering the A subsystem as that formed by the central H_2 of the H_{10} embedded in the rest of the chain, interacting with the H_2.[43,56]

The situation found for the 1b isomer, shown in Figure 6, is analogous to that of the 1a one. The potential for the ground state is reasonably reproduced by the $\mathcal{V}_A(X)$, presenting a well, while when using $\mathcal{V}_A(B)$ the potential curve presents a maximum for 3.5 Å, and for shorter distances it becomes too attractive. For the excited electronic states, the best results are obtained when using the $\mathcal{V}_A(B)$ embedding potential. The quantitative disagreement between the exact results and those obtained with the embedding potential is different for 1a and 1b isomers because the nature of the bond is different, but the qualitative behavior is the same in the two cases. In the two cases two different state-specific embedding potentials are needed to reproduce qualitatively correctly the ground and excited electronic state, and in both cases this may be explained by the differences of the density differences obtained for the ground and excited states, respectively, which constitute the driving force which determines the embedding potential.

Once the reason for the need of state-specific embedding potential is clear, it is important to give a procedure to determine a priori whether or not this is needed. The whole problem consists in that the excitation is nonlocal in A. This could be approximately determined a priori by looking to the virtual orbitals such as the LUMO σ_u orbital of Br_2 in the present case. The electronic configurations and the HOMO−LUMO orbitals of the $H_2O-Br_2(X)$ state are shown in Figure 4. The HOMO orbital is well localized on the Br_2 subsystem. The LUMO orbital, however, has a non-negligible component on the oxygen atom of the H_2O molecule, and as a consequence the excitation cannot be considered as completely localized in A. At this point, it would be very convenient to find a property useful as a quantitative index. A measure of localization might be provided by the projection of the LUMO orbital (the orbital involved in the excitation studied here) on the B subsystem. Future work will focus on this point.

3.3. $(H_2O)_5-Br_2$ Case. The lone pair of the oxygen plays an active role in the bonding of the H_2O-Br_2 complex, modifying also the electronic excitation of Br_2. An interesting question is to what extent this lone pair is also affecting the halogen when it is forming hydrogen bonds with other water molecules. For this purpose, we have studied the cluster formed with five water molecules and a bromine molecule, which has several isomers with similar energies.[3] Here we consider the most stable of them according to ref 3. Structure 5a is characterized by having five water molecules arranged in a slightly distorted pentagon and a bromine molecule above it forming a halogen-bond with the oxygen atom of one water molecule, distorted by the interactions with other hydrogen and oxygen atoms of different water molecules. Each water molecule presents two hydrogen bonds with the two neighboring water molecules in the ring, keeping one lone-pair partially occupied.

Taking A = Br_2 and B = $(H_2O)_5$ the situation is analogous to that reported for H_2O-Br_2: two state-specific embedding

DOI: 10.1021/ct501140p
J. Chem. Theory Comput. 2015, 11, 1155−1164

potentials are needed. Using $\mathcal{V}_A(X)$ the potential of the ground state presents a shallow well of ≈547.5 cm^{-1}, while that obtained using $\mathcal{V}_A(B)$ is very repulsive. On the contrary, the potential curves obtained with $\mathcal{V}_A(X)$ for the two excited electronic states present an unphysical attractive interaction, as it was the case for Br_2−H_2O described above. The excited potential curves obtained with $\mathcal{V}_A(B)$ are more adequate presenting the characteristic repulsive behavior reported for the dimer.

When using two embedding potentials, attention must be paid to properly define the total energies given in eq 9. In each case a different reference E_{tot} and $E_{A,HF}$ is used. $E_{tot,HF}$ here is the HF energy of the whole AB system for the X (denoted by $E_{AB,HF}(X)$) and B ($E_{AB,HF}(B)$) states. The HF energy of the A subsystem for states X or B, using the embedding potentials for states X or B, are denoted by $\mathcal{E}_{HF}^{\mathcal{V}_X}(X)$ and $\mathcal{E}_{HF}^{\mathcal{V}_B}(B)$, respectively. Finally, the *CI* energy of state *i* is denoted by $\mathcal{E}_{CI}^{\mathcal{V}_X}(i)$ and $\mathcal{E}_{CI}^{\mathcal{V}_B}(i)$, depending on the reference density used to calculate the embedding potential. Thus, the energies of the three states considered here obtained using two embedding potentials are given by

$$\begin{aligned} E(X) &= E_{AB,HF}(X) + [\mathcal{E}_{CI}^{\mathcal{V}_X}(X) - \mathcal{E}_{HF}^{\mathcal{V}_X}(X)] \\ E(B) &= E_{AB,HF}(B) + [\mathcal{E}_{CI}^{\mathcal{V}_B}(B) - \mathcal{E}_{HF}^{\mathcal{V}_B}(B)] + D \\ E(C) &= E_{AB,HF}(B) + [\mathcal{E}_{CI}^{\mathcal{V}_B}(C) - \mathcal{E}_{HF}^{\mathcal{V}_B}(B)] + D \end{aligned} \quad (10)$$

where $D = [E_{AB,HF}(B) - E_{AB,HF}(X)]_{R\to\infty}$. D can also be considered as the difference between the *CI* energies of the A subsystem in B and X states, respectively, but here we keep the D defined above for consistency.

Table 1. Vertical Energies, $T_\nu(B) = E(B)-E(X)$ and $T_\nu(C) = E(C)-E(X)$, in cm^{-1} for $R_{Br_2-H_2O} = 3$ Å[b]

method	$T_\nu^5(B)$	$T_\nu^5(C)$	$T_\nu^0(B)$	$T_\nu^0(C)$	$\delta\nu(B)$	$\delta\nu(C)$
RMP2[a]	19755		16605		3150	
CCSD(T)[a]	20508		17920		2588	
CI this work	20067		18430		1637	
CI+Q this work	20756		18218		2542	
$\mathcal{V}(X\&B)$	21139	25983	19031	23772	2108	2211

[a]Reference 3. [b]The superscript indicates the number of water molecules. $\delta\nu = T_\nu^5 - T_\nu^0$ is the energy shift of the vertical transition of the $(H_2O)_5$−Br_2 complex with respect to that of bare Br_2.

In Table 1 are listed the vertical excitation for the B, $T_\nu^5(B)$, and C states, $T_\nu^5(C)$, for the $(H_2O)_5$−Br_2 complex. These T_ν are obtained as the difference between the ground energy using $\mathcal{V}_A(X)$ and the energies of the B and C states obtained using $\mathcal{V}_A(B)$ and MRCI calculations on the bare A subsystem, using the energies defined in eq 10. The two embedding potentials were obtained at the equilibrium geometry of the 5a isomer found in ref 3. To use the same basis and procedures, we estimated the excitation energies by increasing the distance between the Br_2 center of mass and the $(H_2O)_5$ cluster to large intermolecular distances and called them $T_\nu^0(B)$ and $T_\nu^0(C)$ since they correspond to the excitation energies of bare Br_2. The energy shift $\delta_\nu(B) = T_5^\nu(B) - T_\nu^0(B)$ is then compared with the CCSD(T) and RMP2 results obtained in ref 3 for the whole system.

The vertical excitation energies for bare Br_2 are all relatively close for the higher correlated methods, but the RMP2 method leads to a more noticeable underestimation. The shift with respect to the vertical excitation energies of bare Br_2(B), denoted by δ_ν(B) obtained with the two embedding potentials, is smaller than those obtained previously for the whole system using the RMP2 and CCSD(T) methods in ref 3. Given the difference in electronic structure methods we decided to perform new calculations on the Br_2+$(H_2O)_5$ system at the MRCI level which is the correlation level used in the embedding procedure, and the results are shown in Figure 7.

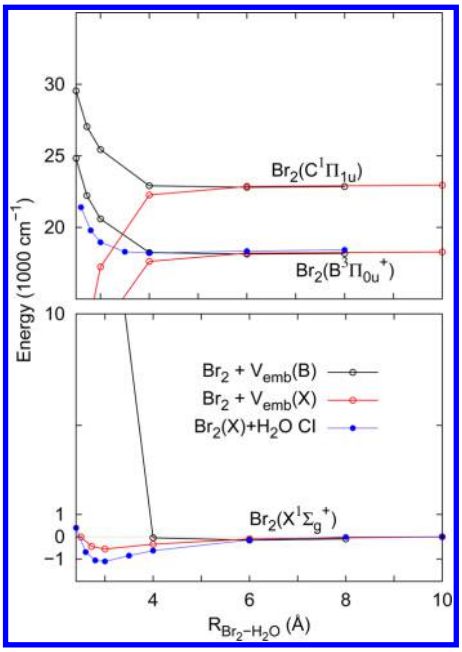

Figure 7. Same as in Figure 3 but for the 5a isomer of $(H_2O)_5$−Br_2, with A = Br_2.

The calculations were based on an active space of 10 electrons in six orbitals corresponding to the 4p atomic shell of Br for the orbital optimization step. This is followed by multireference CI calculations where single and double excitation from the three highest occupied orbitals of each water molecule are additionally allowed. In this way the important dispersion interaction is partially included in the calculations. We see that now the shift at the MRCI+Q level is very similar to that obtained with CCSD(T). The estimate at the MRCI level is smaller due to two factors: an underestimation of the binding energy in the ground state and a larger value of the equilibrium intermolecular distance which reflects in a smaller energy contribution from the repulsive wall in the excited state. Considering the difficulties in accurately estimating electronic shifts the embedding method is promising. Technical problems in converging the MRCI calculations for the excited singlet states precluded us from comparing them with the embedding method, but given the close similarity in electronic structure between the B and C states results can be expected to be analogous to those presented.

The density differences obtained for the ground and excited state of the $(H_2O)_5$−Br_2 complex, $\Delta^0(X)$ and $\Delta^0(B)$, are shown in the top panels of Figure 8. $\Delta^0(X)$ presents a complex sequence of nodes essentially located on the Br_2 but also on the

DOI: 10.1021/ct501140p
J. Chem. Theory Comput. 2015, 11, 1155−1164

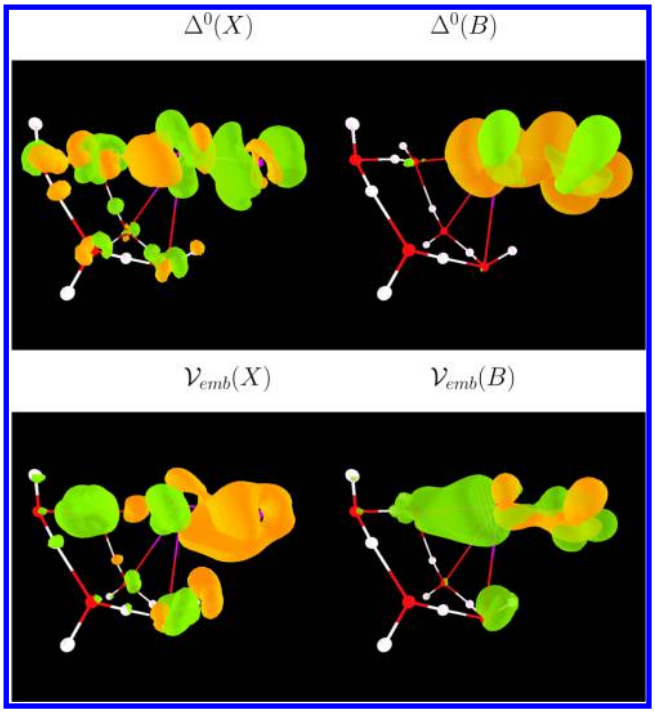

Figure 8. Top panels, density diferences, $\Delta^0(X) = \rho(X) - \rho_A(X) - \rho_B(X)$ and $\Delta^0(B) = \rho(B) - \rho_A(B) - \rho_B(X)$, obtained for the X and B states of the $(H_2O)_5$–Br_2 complex for $R_{Br_2-H_2O}$ = 3 Å, respectively. Bottom panels, are the $\mathcal{V}(X)$ and $\mathcal{V}(B)$ embedding potentials obtained using the corresponding density differences iteratively. Green/orange colors are used to represent possitive/negative values of Δ^0 and $\mathcal{V}$ equisurfaces.

water molecules. This is a clear indication that in the formation of the halogen-bond in the ground X state, the orbitals of the water molecules also participate. On the contrary, $\Delta^0(B)$ is essentially located on the Br_2 molecule. This can be explained by the repulsive nature of the halogen-water interaction on the excited states, which does not allow the two subsystem densities to mix as in the ground electronic state, where they do form a halogen bond. The different density-differences give rise to two different embedding potentials to describe Br_2 in $(H_2O)_5$, since Δ^k is the driving force that gives rise to the $\mathcal{V}(X)$ and $\mathcal{V}(B)$ potentials. Consequently, these two embedding potentials show structures similar to that of Δ^0, but with opposite sign, as explained above. In this case, the oxygen atoms of each water molecule are forming one bond with a hydrogen atom of another water molecule. Thus, one lone pair is still available for forming bonds and consequently interacts strongly with the halogen molecule orbitals.

4. CONCLUSIONS

In this work a DDD-OEP method[43,56] to calculate embedding potentials on an active region A has been slightly modified to be applied in two steps. First, a common and unique embedding potential is defined for the active (A) region and the environment (B), to fulfill the condition discussed by Huang et al.[57] Second, the embedding potentials for A and B are allowed to differ by considering an alternative optimization procedure between A and B separately, as originally proposed.[56] This second step allows for including the polarization in subsystem A induced by the environment B and vice versa. Also, the density difference is considerably reduced by following this method.

It is stressed that the embedding potential is a functional of the density difference, Δ, between the density of the total system AB and the sum of the densities of A and B obtained separately.[43,56] Thus, the density difference acts as a driving force to get the condition $\Delta \rightarrow 0$. For doing that it is clearly stated that the self-repulsion potential obtained from the exchange matrix obtained from Δ plays a crucial role, as proposed previously.[56]

This method is applied to the vertical electronic excitation of Br_2 in water clusters, to the particular cases of 1 and 5 water molecules. It is found that the electronic excitation cannot be reproduced by a single embedding potential for X, B, and C states. The reason is that in the ground state, the LUMO orbital approximately corresponds to that of the bare Br_2 but also has important contributions of the closest water molecules. This is due to the participation of the lone electron pair of water in the formation of the halogen Br_2–H_2O bond. Thus, the water, considered as the environment, also participates in the electronic excitation and cannot be considered to be "inert".

In this situation one possible solution is to include the closest water molecules within the active region to describe the electronic excitation. However, in general environments such as liquid water or clathrates this is impractical since it would involve the inclusion of too many electrons. For example, in dynamical QM/MM calculations of the photochemistry of molecules in liquids or the interface[67] a single water molecule is included in highly correlated calculations of the excited states, but the election of the water molecule may be difficult since more than one may have important contributions. As an alternative, here we propose to use state specific embedding potentials as recently proposed.[42] The results obtained using different embedding potential for the ground and excited electronic states have been compared with accurate results obtained for the whole system, yielding rather good results. This is very promising particularly taking into account that the electronic excitation in Br_2 yields to the repulsive part of the potentials, and small changes yields to rather large variations in energy.

One price to pay, however, arises from the lack of orthogonality between the electronic functions obtained with different embedding potentials, which avoids the calculation of transition moments. For this some more refinements of the method should be investigated.

These methods are then expected to work for the electronic spectroscopy of molecules inside the cages of clathrate hydrates. Some preliminary results have been obtained for the 5^{12} 6^2 clathrate formed by 24 water molecules using the diffraction data of the bromine hydrate TS-I,[6] and the hydrogen atoms were positioned to obtain a low dipole moment cluster using the Buch procedure.[68] As in the cluster, the Br_2 was considered the active subsystem and was separated from all the water molecules of the cage. In this case we could not get convergence when using the triplet state density, and some work should be done to overcome this difficulty; for the moment we consider these as preliminary results. Therefore, using only one single embedding potential obtained for the ground singlet state, we have calculated the excitation energies for the B and C excited electronic states at the MRCI level on subsystem A = Br_2 with the embedding potential. The excitation energies obtained are $T_v(B)$ = 19001 cm^{-1} and $T_v(C)$ = 23814 cm^{-1}. When comparing these results with those

DOI: 10.1021/ct501140p
J. Chem. Theory Comput. 2015, 11, 1155–1164

of the bare Br_2, listed in Table 1, yields to $\delta\nu(B) = -31$ cm^{-1} and $\delta\nu(C) = 42$ cm^{-1}. These values are consistent with recent results obtained using a structured electrostatic model around Br_2.[69] If the use of one single embedding potential is validated, this could be due to the smaller interaction between Br_2 and water molecules in the clathrate by two reasons. First, the oxygen atoms in the clathrate are bound to 4 hydrogen atoms by either covalent or hydrogen bonds, and the lone electron pair is partially saturated to form a new bond with Br_2. Second, the cage considered here is rather large, and the distances between Br_2 and water molecules are rather long. Future work is aimed to verify in more detail the agreement is not fortuitous. The weak dependency of the excitation shifts on the environment densities were also found recently in the study of solvatochromatic shifts in the case of organic chromophores.[70]

AUTHOR INFORMATION

Corresponding Author

*E-mail: octavio.roncero@csic.es.

Notes

The authors declare no competing financial interest.

ACKNOWLEDGMENTS

This work has been supported by the Ministerio de Economía e Innovación under grants Nos. CSD2009-00038 and FIS2011-29596-C02. The calculations have been perfomed in the CESGA computing centre under computing ICTS grants. Support from Conacyt project 128065 for our collaboration is also acknowledged. We acknowledge Prof. R. López for providing us the DAMQT package for the analysis of electronic density[71] and for helping us in using it.

REFERENCES

(1) Goldschleger, I. U.; Kerenskaya, G.; Janda, K. C.; Apkarian, V. A. Polymorphism in Br_2 Clathrate Hydrates. *J. Phys. Chem. Lett.* **2008**, *112*, 787.

(2) Goldschleger, I. U.; Kerenskaya, G.; Senekerimyan, V.; Janda, K. C.; Apkarian, V. A. Dynamical interrogation of the hydration cage of bromine in single crystal clathrate hydrates versus water. *Phys. Chem. Chem. Phys.* **2008**, *10*, 7226.

(3) Bernal-Uruchurtu, M. I.; Hernández-Lamoneda, R.; Janda, K. C. On the Unusual Properties of Halogen Bonds: A Detailed ab Initio Study of X_2-$(H_2O)_{1-5}$ clusters (X = Cl and Br). *J. Phys. Chem. A* **2009**, *113*, 5496.

(4) Kerenskaya, G.; Goldschleger, I. U.; Apkarian, V. A.; Janda, K. C. Spectroscopic Signatures of Halogens in Clathrate Hydrate Cages. 1. Bromine. *J. Phys. Chem. A* **2006**, *110*, 13792.

(5) Pauling, L.; Marsh, R. E. The structure of Chlorine hydrate. *Proc. Natl. Acad. Sci. U. S. A.* **1952**, *38*, 112.

(6) Udachin, K.; Enright, G.; Ratcliffe, C.; Ripmeester, J. Structure, stoichiometry, and morphology of bromine hydrate. *J. Am. Chem. Soc.* **1997**, *119*, 11481.

(7) Udachin, K. A.; Alavi, S.; Ripmeester, J. A. Water-Halogen Interactions in Chlorine and Bromine Clathrate Hydrates: An Example of Multidirectional Halogen Bonding. *J. Phys. Chem. C* **2013**, *117*, 14176.

(8) Runge, E.; Gross, E. K. U. Density-functional theory for time-dependent systems. *Phys. Rev. Lett.* **1984**, *52*, 997.

(9) Jacquemin, D.; Mennucci, B.; Adamo, C. Excited-state calculations with TD-DFT: from benchmarks to simulations in complex environments. *Phys. Chem. Chem. Phys.* **2011**, *13*, 16987.

(10) Humbel, S.; Sieber, S.; Morokuma, K. The IMOMO method: integration of different levels of molecular orbital approximations for geometry optimization of large systems: Test for *n*-butane conformation and S_N2 reaction: RCl+Cl$^-$. *J. Chem. Phys.* **1996**, *105*, 1959.

(11) Svensson, M.; Humbel, S.; Froese, R.; Matsubara, T.; Sieber, S.; Morokuma, K. ONIOM: a multilayered integrated MO+MM method for geometry optimization and single point energy predictions. *J. Phys. Chem.* **1996**, *100*, 19357.

(12) Senn, H. M.; Thiel, W. QM/MM methods for biological systems. *Top. Curr. Chem.* **2007**, *268*, 173.

(13) Sokol, A. A.; Bromley, S. T.; French, S. A.; Catlow, C. R. A.; Sherwood, P. *Int. J. Quantum Chem.* **2004**, *99*, 695.

(14) Friesner, R. A.; Guallar, V. Ab initio quantum chemical and mixed quantum mechanics/molecular mechanics (QM/MM) for studying enzimatic catalysis. *Annu. Rev. Phys. Chem.* **2005**, *56*, 389.

(15) Schwabe, T.; Sneskov, K.; Olsn, J. M. H.; Kongsted, J.; Christiansen, O.; Hattig, C. *J. Chem. Theory Comput.* **2012**, *8*, 3274.

(16) Gomes, A. S. P.; Jacob, C. R. Quantum-chemical embedding methods for treating local electronic excitations in complex chemical systems. *Annu. Rep. Prog. Chem., Sect. C: Phys. Chem.* **2012**, *108*, 222.

(17) Cortona, P. Self-consistently determined properties of solids without band-structure calculations. *Phys. Rev. B* **1991**, *44*, 8454.

(18) Stefanovich, E. V.; Truong, T. N. Embedded density functional approach for calculations of adsorption on ionic crystals. *J. Chem. Phys.* **1996**, *104*, 2946.

(19) Wesolowski, T. A.; Warshel, A. Frozen Density Functional Approach for ab initio Calculations in Solvated molecules. *J. Phys. Chem.* **1993**, *97*, 8050.

(20) Wesolowski, T. A.; Weber, J. Kohn-Sham equations with constrained electron density: an iterative evaluation of the ground-state electron density of interacting molecules. *Chem. Phys. Lett.* **1996**, *248*, 71.

(21) Neugebauer, J.; Louwerse, M. J.; Belanzoni, P.; Wesolowski, T. A.; Baerends, E. J. Modeling solvent effects on electron-spin-resonance hyperfine couplings by frozen-density embedding. *J. Chem. Phys.* **2005**, *123*, 114101.

(22) Neugebauer, J.; Jacob, C. R.; Wesolowski, T. A.; Baerends, E. J. An explicit quantum mechanical method for modeling large solvation shells applied to aminocoumarin C151. *J. Phys. Chem. A* **2005**, *109*, 7805.

(23) Jacob, C. R.; Neugebauer, J.; Jensen, L.; Visscher, L. Comparison of frozen-density embedding and discrete reaction field solvent models for molecular properties. *Phys. Chem. Chem. Phys.* **2006**, *8*, 2349.

(24) Wesolowski, T. A. Embedding a multideterminantal wave function in an orbital-free environment. *Phys. Rev. A* **2008**, *77*, 012504.

(25) Dulak, M.; Wesolowski, T. A. Nonlinearity of the Bifunctional of the Nonadditive kinetic energy: Numerical consequences in orbital-free embedding calculations. *J. Chem. Theory Comput.* **2006**, *2*, 1538.

(26) Wesolowski, T. A. Density functional theory with approximate kinetic energy functionals applied to hydrogen bonds. *J. Chem. Phys.* **1997**, *106*, 7178.

(27) Tran, F.; Wesolowski, T. A. Link between the kinetic- and exchange-energy functionals in the generalized gradient approximation. *Int. J. Quantum Chem.* **2002**, *89*, 441.

(28) Jacob, C. R.; Beyhan, S. M.; Visscher, L. Exact functional derivative of the nonadditive kinetic-energy bifunctional in the long-distance limit. *J. Chem. Phys.* **2007**, *126*, 234116.

(29) Fux, S.; Jacob, C. R.; Neugebauer, J.; Visscher, L.; Reiher, M. Accurate frozen-density embedding potentials as a first step towards a subsystem description of covalent bonds. *J. Chem. Phys.* **2010**, *132*, 164101.

(30) Casida, M. E.; Wesolowski, T. A. TD-DFT in FDE. *Int. J. Quantum Chem.* **2004**, *96*, 577.

(31) Neugebauer, J. Couplings between electronic transitions in a subsystem formulation of time-dependent density functional theory. *J. Chem. Phys.* **2007**, *126*, 134116.

(32) Neugebauer, J.; Curutchet, C.; Muñoz-Losa, A.; Mennucci, B. A subsystem TDDFT approach for solvent screening effects on excitation energy transfer couplings. *J. Chem. Theory Comput.* **2010**, *6*, 1843.

DOI: 10.1021/ct501140p
J. Chem. Theory Comput. 2015, 11, 1155−1164

(33) Huang, C.; Libisch, F.; Peng, Q.; Carter, E. A. Time-dependent potential-functional embedding theory. *J. Chem. Phys.* **2014**, *140*, 124113.
(34) Govind, N.; Wang, Y. A.; Carter, E. A. Electronic calculations by first-principles density-based embedding of explicitly correlated systems. *J. Chem. Phys.* **1999**, *110*, 7677.
(35) Klüner, T.; Govind, N.; Wang, Y. A.; Carter, E. A. Periodic density functional embedding theory for complete active space self-consistent field and configuration interaction calculations: ground and excited states. *J. Chem. Phys.* **2002**, *116*, 42.
(36) Huang, P.; Carter, E. A. Self-consistent embedding theory for locally correlated configuration interaction wave functions in condensed matter. *J. Chem. Phys.* **2006**, *125*, 084102.
(37) Huang, P.; Carter, E. A. Advances in correlated electronic structure methods for solids, surface and nanostructures. *Annu. Rev. Phys. Chem.* **2008**, *59*, 261.
(38) Hofener, S.; Gomes, A. S. P.; Visscher, L. Molecular properties via a subsystem density functional theory formulation: A common framework for electronic embedding. *J. Chem. Phys.* **2012**, *136*, 044104.
(39) Goodpaster, J. D.; Barnes, T. A.; Manby, F. R., III; Miller, T. F. Density functional theory embedding for correlated wavefunctions: Improved methods for open-shell systems and transition metal complexes. *J. Chem. Phys.* **2012**, *137*, 224113.
(40) Libisch, F.; Huang, C.; Carter, E. A. Embedded correlated wavefunction schemes: theory and applications. *Acc. Chem. Res.* **2014**, *47*, 2768.
(41) Goodpaster, J. D.; Barnes, T. A.; Manby, F. R., III; Miller, T. F. Accurate and systematically improvable density functional theory embedding for correlated wavefunctions. *J. Chem. Phys.* **2014**, *140*, 18A507.
(42) Daday, C.; König, C.; Valsson, O.; Neugebauer, J.; Filippi, C. State-specific embedding potentials for excitation-energy calculations. *J. Chem. Theory Comput.* **2013**, *9*, 2355.
(43) Roncero, O.; de Lara-Castells, M. P.; Villarreal, P.; Flores, F.; Ortega, J.; Paniagua, M.; Aguado, A. An inversion technique for the calculation of embedding potentials. *J. Chem. Phys.* **2008**, *129*, 184104.
(44) Zhao, Q.; Morrison, R. C.; Parr, R. G. From electron densities to Kohn-Sham kinetic energies, orbital energies, exchange-correlation potentials. *Phys. Rev. A* **1994**, *50*, 2138.
(45) Goodpaster, J. D.; Ananth, N.; Manby, F. R., III; Miller, T. F. Exact nonadditive kinetic potentials for embedding density functional theory. *J. Chem. Phys.* **2010**, *133*, 084103.
(46) Wu, Q.; Yang, W. A direct optimization method for calculating density functionals and exchange-correlation potential from electron densities. *J. Chem. Phys.* **2003**, *118*, 2498.
(47) Talman, J. D.; Shadwick, W. F. Optimized effective atomic central potentials. *Phys. Rev. A* **1976**, *14*, 36.
(48) Almbladh, C. O.; Pedroza, A. C. Density-functional exchange-correlation potentials and orbital eigenvalues for light atoms. *Phys. Rev. A* **1984**, *29*, 2322.
(49) van Leeuwen, R.; Baerends, E. J. Exchange-correlation potential with correct asymptotic behavior. *Phys. Rev. A* **1994**, *49*, 2421.
(50) Gritsenko, O. V.; van Leeuwen, R.; Baerends, E. J. Molecular Kohn-Sham exchange-correlation potential from the correlated ab initio electron density. *Phys. Rev. A* **1995**, *52*, 1870.
(51) Tozer, D. J.; Handy, N. C.; Palmieri, P. Constrained minimizations for the calculation of Kohn-Sham and natural orbitals. *Mol. Phys.* **1997**, *91*, 567.
(52) Chan, G. K. L.; Handy, N. C. Kinetic-energy, density scaling, and homogeneity relations in density-functional theory. *Phys. Rev. A* **1999**, *59*, 2670.
(53) Gál, T. First-degree homogeneous N-particle noninteracting kinetic-energy functionals density. *Phys. Rev. A* **2001**, *64*, 062503.
(54) Yang, W.; Wu, Q. Direct method for optimized effective potentials in density-functional theory. *Phys. Rev. Lett.* **2002**, *89*, 143002.
(55) Manby, F. R.; Stella, M.; Goodpaster, J. D., III; Miller, T. F. A simple, exact density-functional theory embedding scheme. *J. Chem. Theory Comput.* **2012**, *8*, 2564.
(56) Roncero, O.; Zanchet, A.; Villarreal, P.; Aguado, A. A density-division embedding potential inversion technique. *J. Chem. Phys.* **2009**, *131*, 234110.
(57) Huang, C.; Pavone, M.; Carter, E. A. Quantum mechanical embedding theory based on a unique embedding potential. *J. Chem. Phys.* **2011**, *134*, 154110.
(58) Cohen, M. H.; Wasserman, A. On the Foundations of Chemical Reactivity Theory. *J. Phys. Chem. A* **2007**, *111*, 2229.
(59) Elliot, P.; Cohen, M. H.; Wasserman, A.; Burke, K. Density Functional Partition Theory with Fractional Occupations. *J. Chem. Theory Comput.* **2009**, *5*, 827.
(60) Mosquera, M. A.; Jensen, D.; Wasserman, A. Fragment-Based Time-Dependent Density Functional Theory. *Phys. Rev. Lett.* **2013**, *111*, 023001.
(61) MOLPRO is a package of ab initio programs designed by H.-J. Werner and P. J. Knowles and with contributions from J. Almlöf, R. D. Amos, A. Berning, M. J. O. Deegan, F. Eckert, S. T. Elbert, C. Hampel, R. Lindh, W. Meyer, A. Nicklass, K. Peterson, R. Pitzer, A. J. Stone, P. R. Taylor, M. E. Mura, P. Pulay, M. Schütz, H. Stoll, T. Thorsteinsson, D. L. Cooper version 2012.
(62) Dunning, T. H., Jr. Dunning electronic basis set functions −1. *J. Chem. Phys.* **1989**, *90*, 1007.
(63) Bergner, A.; Dolg, M.; Kuechle, W.; Stoll, H.; Preuss, H. Ab initio energy-adjusted pseudopotentials for elements of groups 13−17. *Mol. Phys.* **1993**, *80*, 1431.
(64) Hernández-Lamoneda, R.; Sanz-Sanz, C.; Roncero, O.; Pio, J. M.; Taylor, M. A.; Janda, K. C. A theoretical study on electronic predissociation in the $NeBr_2$ van der Waals molecule. *Chem. Phys.* **2012**, *399*, 86.
(65) Legon, A. C. Prereactive complexes of dihalogens XY with Lewis bases B in the gas phase: a systematic case for the halogen analogue B···XY of the hydrogen bond B···HX. *Angew. Chem., Int. Ed.* **1999**, *38*, 2686.
(66) Langreth, D. C.; Dion, M.; Rydberg, H.; Schröder, E.; Hyldgaard, P.; Lundqvist, B. I. van der Waals density functional theory with applications. *Int. J. Quantum Chem.* **2004**, *101*, 599.
(67) Anglada, J.; Martins-Costa, M.; Ruiz-López, M. F.; Francisco, J. Spectroscopic signatures of ozone at the airwater interface and photochemistry implications. *Proc. Natl. Acad. Sci. U. S. A.* **2014**, *111*, 11618.
(68) Buch, V.; Sandler, P.; Sadlej, J. Simulations of H_2O Solid, Liquid, and Clusters, with an Emphasis on Ferroelectric Ordering Transition in Hexagonal Ice. *J. Phys. Chem. B* **1998**, *102*, 8641.
(69) Bernal-Uruchurtu, M. I.; Janda, K. C.; Hernández-Lamoneda, R. Motion of Br_2 molecules in Clathratecages. A computational study of the dynamic effects on its spectroscopic behavior. *J. Phys. Chem. A* **2015**, *119*, 452.
(70) Humbert-Droz, M.; Zhou, X.; Shedge, S. V.; Wesoloski, T. A. How to choose the frozen density in Frozen density embedding theory-based numerical simulations of local excitations? *Theor. Chem. Acc.* **2014**, *133*, 1405.
(71) López, R.; Fernández-Rico, J.; Ramírez, G.; Ema, I.; Zorrilla, D. DAMQT: a package for the analysis of electron density in molecules. *Comput. Phys. Commun.* **2009**, *180*, 2−5.

DOI: 10.1021/ct501140p
J. Chem. Theory Comput. 2015, 11, 1155−1164